Radiation effects and ecological processes in a freshwater microcosm

Hevrøy, T.H.[1,2*], A.-L. Golz[3*], L. Xie[4], E.L. Hansen[1,2], C. Bradshaw[3]

[1]Norwegian Radiation Protection Authority, Grini næringspark 13, 1361 Østerås, Norway
[2]CERAD Centre of Excellence for Environmental Radioactivity, P.O. Box 5003, NO-1432 Ås, Norway
[3]Department of Ecology, Environment and Plant Sciences, Stockholm University, 10691, Stockholm, Sweden
[4]Norwegian Institute for Water Research, Gaustadalleen 21, 0349, Oslo, Norway

*Shared first and corresponding authorship
Email: Tanya.Hevroy@nrpa.no
anna-lea.golz@su.se

Abstract

Ecosystem response to gamma radiation exposure depends on the different species sensitivities and the multitude of direct and indirect pathways by which individual organisms can be affected, including the potential for complex interactions across multiple trophic levels. In this study, multi-species microcosms were used to investigate effects of ionizing radiation in a model freshwater ecosystem, including endpoints at both structural and functional levels and ecological interactions. Microcosms were exposed for 22 days to a gradient of gamma radiation with four dose rates from 0.72 to 19 mGy h^{-1}, which are within the range of those seen at contaminated sites. Results showed significant dose related effects on photosynthetic parameters for all macrophyte species. No significant effects of radiation were observed for the consumers in the microcosms, however trends indicate the potential for longer-term effects. We also witnessed a different response of *Daphnia magna* and *Lemna minor* compared to previous single-species studies, illustrating the importance of multispecies studies, which aim to encompass systems more realistic to natural ecosystems. Microcosms allowed us to isolate specific relationships between interacting species in an ecosystem and test the effects of radiation on them, both direct and indirect. In addition, the ecological pathways and processes, and the experimental design itself, was central to understanding the results we witnessed. This type of study is important for radioecology research that has been very much limited to high dose rates and single species studies. This approach to radioecology has been strongly promoted in recent decades and, to our knowledge, this is the first microcosm study performed at dose rates similar to those at contaminated field sites.

Keywords: microcosm, gamma radiation, ecosystem approach, species interactions, indirect effects[1]

Abbreviations: **øPSII**, maximum quantum efficiency of photosystem II; **ETR**, photosynthetic electron transport rate; **qP**, photochemical quenching coefficient; **qN**, non-photochemical quenching coefficient; **ROS**, reactive oxygen species; **LOP**, lipid peroxidation; **TBARS**, thiobarbituric acid reactive substances; **TBA**, thiobarbituric acid; **TCA**, trichloroacetic acid; **MDA**, malondialdehyde; **GEP**, gross ecosystem production; **NEP**, net ecosystem production; **R**, ecosystem respiration; **TPP**, total pelagic primary production; **BAC**, pelagic bacterial production[1]

Introduction

To understand an ecosystem's response to anthropogenic stress, an understanding of the underlying ecological processes is required to untangle the full extent of direct and indirect effects. Direct effects are most commonly expressed and measured on an individual compartment of an ecosystem while indirect effects are mediated or transmitted through interacting biotic and abiotic compartments of the ecosystem and may not be immediately apparent, although they are common (Fleeger, et al. 2003). Extensive evidence for the important role of ecological processes in determining net ecosystem effects to anthropogenic stressors has led several authors to call for more consideration of community ecology (Relyea and Hoverman 2006; Rohr, et al. 2006) or an ecosystem approach to ecotoxicology (Beketov and Liess 2012; Preston 2002). Similar calls have been made within the radioecology community (Bradshaw, et al. 2014; Bréchignac, et al. 2012; 2016; IUR 2002). However, there is still a significant lack of studies using this approach in radioecological research (Bréchignac, et al. 2016). Today, radiation protection and risk assessments are mainly based on the "Reference Animals and Plants" (RAPs) approach, which uses selected species from various ecological compartments in both terrestrial and aquatic environments (ICRP 2007; Pentreath 2005). However, the ICRP (2007) also states that protection of the environment should aim "…to protect the health and status of natural habitats and communities, and ecosystems", a goal that requires an ecosystem approach with ecological endpoints. The RAPs approach has been criticised for its reductionism in that the selected species cover only a limited part of the natural world, focusing on organism-level endpoints and entirely ignoring the ecosystem level effects (Brèchignac and Doi 2009), leading to a mismatch between the stated protection goal and the approach used to reach that goal (Bradshaw, et al. 2014).

Radiation studies on impacts of radiation on non-human biota have mostly been focused on single species studies or field studies at nuclear accident sites like Chernobyl, Mayak and Fukushima. Most laboratory studies that examine impacts on biota have used external acute exposures of gamma radiation to investigate biological endpoints at the level of individual organisms or lower (Copplestone, et al. 2008) and are therefore lacking in ecological relevance. However, the few studies that have been conducted using chronic exposures to external gamma radiation provide some insight about the doses or dose rates at which effects at sublethal endpoints can be expected. For example; reproductive success has been seen to be impaired in Daphnia magna at 0.38 mGy h-1 (Gilbin, et al. 2008), 3.2 mGy h-1 for the polychaete Ophryotrocha diadema (Knowles and Greenwood 1997) and 10 mGy h-1 for the gastropod Physa heterostropha (Cooley 1973). Additionally, 4.7 mGy h-1 negatively affected D. magna body length and growth (Parisot, et al. 2015), and oxygen consumption in D. magna decreased at circa 31 mGy h-1 external gamma exposure (Gilbin, et al. 2008). Even fewer relevant studies are available for plants, particularly aquatic plants, but dose-dependent growth inhibition and significant oxidative stress responses were exhibited in Lemna minor at ≥ 27 mGy h-1 (Van Hoeck, et al. 2015). The phytoplankton Chlamydomonas reinhardtii showed a range of photosynthetic responses at ≥ 235 mGy h-1 and reactive oxygen species (ROS) production at ≥ 4.5 mGy h-1 (Gomes, et al. 2017). The terrestrial plant Arabidopsis thaliana showed decreased root, leaf and stem biomass at exposures of 0.08 - 2.34 mGy h-1 and a 10% growth rate reduction at 0.06 - 0.08 mGy h-1 (Vandenhove, et al. 2010). Field investigations have shown that the structure and function of ecosystems change with increasing dose (Alexakhin,

et al. 1994; Amiro and Sheppard 1994). In many cases, ecological processes have caused indirect effects (Geras'kin, et al, 2016), for example, the replacement of forest by grass in the Chernobyl Exclusion Zone due to changes to soil quality and microclimate (Geras' kin, et al. 2008) and the dominance of cyanobacteria in contaminated lakes in Mayak due to reduced competition and predation (Pryakhin, et al. 2016). One study (Garnier-Laplace, et al. 2013) compared results from laboratory experiments with Chernobyl field work on terrestrial biota and found that species in their natural environment appeared to be more sensitive to radiation (by a factor of eight). However, other studies show a lack of apparent effects on aquatic invertebrate communities in Chernobyl lakes (Murphy, et al 2011, Fuller, et al 2018; estimated external dose rates in the range of 0.1 – 30 mGy h-1). (Polikarpov 1998) suggested that there is a "zone of ecological masking" in the field, in the exposure range of 0.006 – 0.46 mGy h-1, where radiation effects may occur in individuals but may be masked by other processes occurring in populations or ecosystems. A difficulty with field studies is thus untangling these confounding factors and uncontrolled variables, which can make it difficult to interpret results (Garnier-Laplace, et al. 2006; Garnier-Laplace, et al. 2013; Geras'kin, et al. 2016).

To better discern effects of a contaminant in populations, communities and ecosystems, ecotoxicology studies have commonly used multispecies experiments, often termed microcosms or mesocosms (Clements and Kiffney 1994; Fleeger, et al. 2003; Preston 2002). Micro- and mesocosms are experimental ecosystems of any habitat type, containing multiple species, often from several trophic levels, which can investigate a range of ecological endpoints (Odum 1985). They provide a bridge between laboratory and field studies, retaining some of the natural variation of field studies, with a greater control of conditions and variables, as well as replication, and are therefore an extremely useful tool to investigate how ecosystems respond to stress (Beyers and Odum 1993). Microcosms are a way to simulate the complexity of ecosystems by including multiple species that interact with each other and their abiotic surroundings, thus allowing for the inclusion and/or exploration of indirect effects.

In radioecology, microcosms have mainly been used to illustrate transfer of radionuclides (Fritsch, et al. 2008; Tuovinen, et al. 2016; Yousef, et al. 1975) and their use in studying ecosystem effects have been limited. Microcosm effects studies using exposure to ionizing radiation have used high doses and/or dose rates (e.g., 1-5000 Gy h-1). Numerous microcosm studies have investigated the indirect effects of ionizing radiation in aquatic communities with more than one trophic level (Ferens and Beyers, 1972; Fuma, et al. 1998, 2009, 2010, 2012). However, these studies used acute high doses of radiation (up to 5000 Gy) and communities dominated by microbes, which are known to be highly radiation resistant (Shukla, et al. 2017). Brechignac (2003) argued the need for investigations of population and ecosystem relevant endpoints at dose levels of concern, i.e. dose rates corresponding to real-life scenarios, such as nuclear accidents (Fukushima, Chernobyl – (Geras'kin, 2016)), nuclear waste spills (Mayak – (Pryakhin, et al. 2016)) or nuclear spent fuel canisters (Pitonzo, et al. 1999). It is estimated that in the acute phase (first 20 days) of the Chernobyl accident, in the local area, absorbed dose rates to pine trees from gamma emitters reached up to 20 Gy d-1 (UNSCEAR 2008), equivalent to more than 830 mGy h-1. In the cooling pond, estimated absorbed dose rates to aquatic biota in the acute phase reached up to 400 mGy d-1 (17 mGy h-1) for benthic organisms (UNSCEAR 2008), and up to 100 mGy d-1 (4 mGy h-1) for macroalgae (UNSCEAR 2008). Following the Fukushima accident, absorbed dose rates for marine birds and

macroalgae ranged from 8 to 170 mGy h-1 (Garnier-Laplace, et al. 2011), and predicted absorbed dose rates to marine life (fish, macroalgae and molluscs) ranged from 1 to 10 mGy h-1 in the intermediate phase (first two months) (Strand, et al. 2014).

In this paper we present results from an experiment where freshwater microcosms, containing multiple species from several trophic levels, were exposed to absorbed dose rates from external gamma radiation in the range of 0.72 to 19 mGy h-1. Although these dose rates are orders of magnitude larger than would be expected from routine releases, they are within the range of dose rates measured in the acute to intermediate phase of nuclear accident scenarios such as those mentioned above, and they are within the range of dose rates where previous studies have found ecologically relevant effects on species similar to the community used in this study. In this study, we have measured structural and functional endpoints at different levels of biological organisation to get a better understanding of the effect of radiation on an aquatic ecosystem. To our knowledge, this is the first microcosm study using ionising radiation at this range of dose rates. The aims were to:

1. investigate the effects of ionizing radiation on a model aquatic ecosystem
2. investigate the pathways and interactions between species and components of the ecosystem

2. Material and methods

The species included in the microcosms represented a freshwater environment, and included some species which have been used in radiation studies before (in single species tests) as well as species that can be found in Nordic freshwater ecosystems (Fig. 1). The experiments were conducted at the FIGARO Co-60 gamma irradiation facility in Norway (Hansen et al., 2018) over 22 days (11/10/2016 to 01/11/2016) with a total beam-on exposure time of 466 hours.

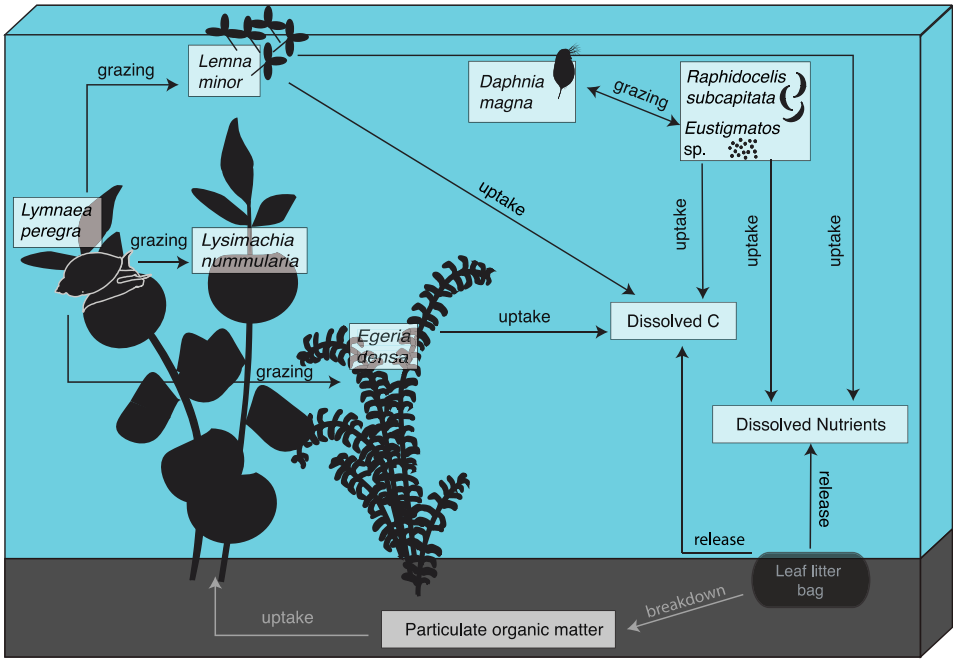

Figure 1. Conceptual model of the NORCO microcosm, illustrating each species and component of the aquatic ecosystem and the ecological interactions between species, and the between species and different components of the microcosm. Solid lines = trophic transfer and dotted line = excretion/ decay.

2.1 Microcosm setup

The microcosms were assembled using artificial freshwater, a 50% diluted modified WC media (Guillard and Lorenzen 1972), sediment, two phytoplankton species (*Raphidocelis subcapitata* and *Eustigmatos magnus*), one zooplankton species (*Daphnia magna*), three plant species (*Lemna minor*, *Lysimachia nummularia* and *Egeria densa*), one gastropod species (*Lymnaea peregra*) and litter bags containing leaves from four Nordic tree species. The species were not selected from sterile laboratory cultures, but were obtained from semi-natural conditions, to allow the establishment of natural microbial communities; this probably also resulted in the introduction of some additional phytoplankton species. The experimental containers were 20 cm x 20 cm x 10 cm (inner dimensions) Plexiglas containers (wall thickness 0.6 cm). Six days before the start of the exposure, the containers were thoroughly rinsed and then filled with 3.8 L of artificial freshwater. Then, we added 630 g of pre-washed sediment (red sand; grain size 0.33 mm). We roughly followed the guidelines for Standard Aquatic Microcosms of Taub et al. (1989) to reduce variability between microcosms. Taub et al. (1989) recommends adding the different components of a microcosm (first phytoplankton and then grazers) over a 4 day period, allowing for 3 days stabilization before starting the experiment. Our communities were gradually assembled over 4 days, allowing three days of stabilization prior to the start of the exposure (Fig. 2). Two rooted macrophytes, *L. nummularia* and *E. densa*, were cut into 5 and 11 cm long pieces, respectively. The fresh weight of the shoots was recorded. After planting two shoots of each macrophyte, 44-48 fronds of *L. minor* were added. Next, 12 *D. magna* (6 "big" 1.97 ± 0.31 mm and six "small"; 0.94 ± 0.06 mm) and four *Lymnaea peregra* were added. *L. peregra* individuals were weighed and measured following OECD guidelines for *L. stagnalis* (OECD 2008). To ensure that phytoplankton abundances were above the incipient limiting level of *D. magna*, 0.5 mg C/L of *R. subcapitata* and 0.25 mg C/L of *E. magnus* (OECD 2008) were added at the start and weekly throughout the experiment. Measurements of carbon concentrations were based on chlorophyll a concentrations using a previously determined relationship between fluorescence (chlorophyll µg / L) and carbon content per cell from dilution series. To measure benthic bacterial activity (degradation of organic matter) within the microcosms, leaf litter bags comprising teabags filled with a known dry weight of leaves of 4 Nordic tree species (birch, maple, willow and oak, dried at 50°C) were placed on the sediment surface.

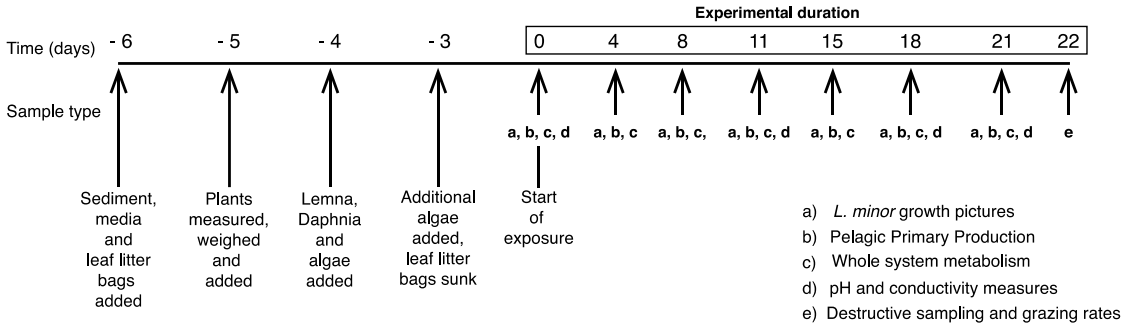

Figure 2. Timeline of construction and stabilization of microcosms, followed by experimental period, and endpoints collected at each time period.

2.2 Experimental setup and irradiation

The exposures were conducted in a climate controlled exposure hall with a Co-60 source at one end (Hansen et al., 2019, Lind et al., 2019). The setup consisted of a total of 19 microcosms, out of which 14 were distributed between four dose rate levels

while five unexposed control microcosms were placed behind lead shielding (Fig. 3). The climate chamber was set to 18 °C, with each microcosm receiving light from LED light sources (c. 1200 lux) on a 16-h light:8-h dark cycle. Both light and temperature were monitored throughout the experiment using temperature and light loggers (HOBO Pendant® Data Logger). The Co-60 source provided gamma irradiation at nominal energies of 1.17 and 1.33 MeV. Microcosms were placed with their front face at 196.2 cm, 315.7 cm, 640.7 cm and 1015.7 cm to the vertical plane containing the Co-60 source focus. Average air kerma rates in air on the central field axis at these distances to the source were 22.1 mGy h^{-1}, 8.46 mGy h^{-1}, 2.03 mGy h^{-1} and 0.80 mGy h^{-1}, respectively (relative uncertainty 3.2%, Hansen et al., 2019). Both control and exposed microcosms were rotated at three time points during the experiment between positions at each dose level in order to average out variation in air kerma rates and potential experimental design effects between positions.

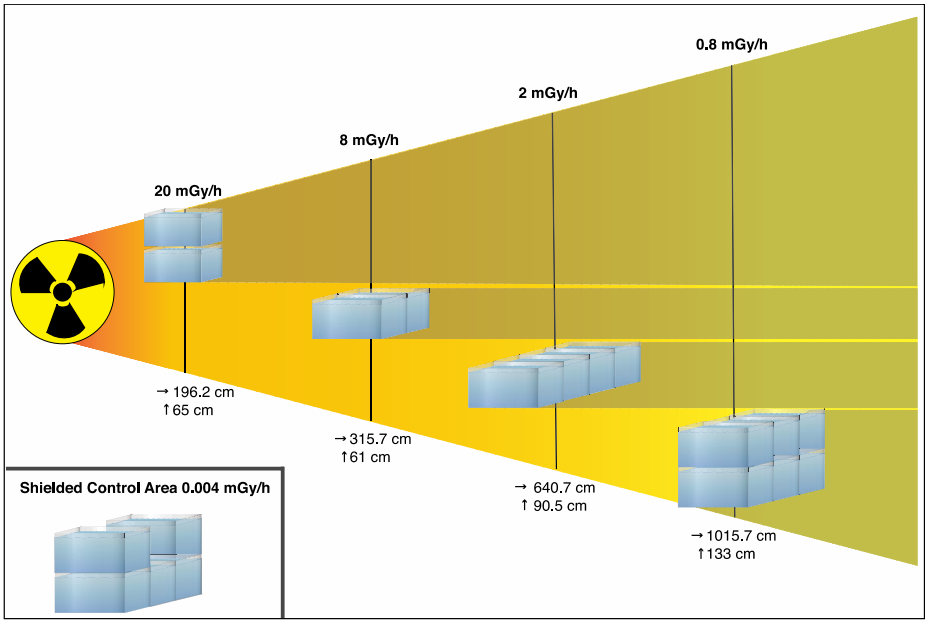

Figure 3. Conceptual set up of the microcosms within the irradiation chamber, illustrating nominal dose rates.

2.3 Dosimetry

The dosimetry was conducted according to the guidelines of a newly developed exposure characterization and dosimetry framework for FIGARO (Hansen et al., 2019). The exposure setup was planned based on reference measurements of air kerma rates by the Secondary Standard Dosimetry Laboratory (SSDL) at the Norwegian Radiation Protection Authority (Bjerke and Hetland 2014) and verified by measurements of air kerma rates with nanoDot dosimeters (Landauer, Inc., Greenwood, IL).

The dosimetry framework for FIGARO includes a Geant4 (Agostinelli, et al. 2003; Allison, et al. 2006; Allison, et al. 2016) Monte Carlo radiation transport model of the exposure hall and source that is used for simulating air kerma rates and absorbed dose rates to experiments. A Geant4 model of the exposure setup for microcosms has been described in Hansen et al. (2019) for simulating average whole-setup absorbed dose rates to water for each microcosm. In the current work, we also simulated absorbed dose rates to plants that occupy the midplane of microcosms (*E. densa* and *L. nummularia*) and to plants that occupy the water surface (*L. minor*). We estimated that absorbed dose rates to *D. magna* are well approximated by the average absorbed dose rates to water for each microcosm because *D. magna* utilise the full microcosm volume. All organisms were modelled with the same density and composition as water.

The simulated average beam-on absorbed dose rates to water for each microcosm (referred to as average dose rates in later sections) ranged from 19 mGy h^{-1} (for microcosm 19 at the highest dose level) to 0.72 mGy h^{-1} (for microcosm 20 at the lowest dose level). Accumulated absorbed doses to water (referred to as accumulated doses in later sections) ranged from 8.8 Gy (microcosm 19) to 0.33 Gy (microcosm 20). Estimated average absorbed dose rates to plants that occupied the midplane of microcosms (*E. densa* and *L. nummularia*) deviated from the average absorbed dose rates to water by a few percent (Table 1). This is because a broad Co-60 gamma field gives rise to depth dose curves that decrease in an approximately linear way with the water depth (McKenzie 1995). Estimated average absorbed dose rates to plants that occupied the water surface (*L. minor*) varied more relative to the average absorbed dose rates to the whole microcosms (Table 1). This is a result of variations in the FIGARO gamma field strength which, particularly in the vertical direction (Hansen, et al. 2019), affects microcosms depending on where they are in the field. The effect is most severe for microcosms that are close to the source, and less severe for microcosms that are placed further back in the exposure hall, where their surface areas occupy a smaller proportion of the field. In the following sections, measured endpoints are related to the average absorbed dose rates to water (for simplicity, average dose rates) for each microcosm.

Table 1. Simulated beam-on absorbed dose rates and accumulated doses to water for the whole microcosms and for plants at the midplane of microcosms or at the water surface. Relative standard uncertainties are estimated to 8% on the absorbed dose rates and on accumulated doses (Hansen et al, in review) and data are only reported when relative uncertainties from repeated simulations were at or below 3% (for the remaining positions, this can be achieved in the future by increasing the number of runs and/or the number of simulated photons per run). The minimum and maximum dose rates show the range in dose rates between the different positions that a microcosm occupied internally at a dose level.

dose level	cosm	whole-microcosm doses to water				doses to plants	
						midplane	surface
		accumulated doses	dose rates				
			minimum	maximum	average		
		[Gy]	[mGy h^{-1}]				
1	19	8.8	17.0	20.0	19.0	20.0	14.0
	2	8.6	17.0	20.0	18.0	20.0	13.0
2	4	3.7	7.6	8.1	7.9	8.2	6.8
	9	3.6	7.6	8.1	7.8	8.2	6.8
3	13	0.81	1.5	1.8	1.7	1.8	-
	22	0.80	1.5	1.8	1.7	1.8	-
	14	0.78	1.5	1.8	1.7	1.7	-
	5	0.78	1.5	1.8	1.7	1.7	-
4	11	0.34	0.72	0.74	0.73	0.75	-
	15	0.34	0.72	0.75	0.73	0.76	-
	18_or_8b	0.34	0.72	0.74	0.73	0.76	-
	6	0.34	0.70	0.74	0.72	0.74	-
	18_or_8a	0.33	0.69	0.73	0.72	0.74	-
	20	0.33	0.69	0.73	0.72	0.75	-
controls		2e-3	-		4e-3	-	

2.4 Sampling during the experiment

Pelagic primary and bacterial production, whole system metabolism as well as pH, temperature and conductivity, were measured at multiple time points during the experiment (Fig. 2).

Whole system metabolism was determined by measuring changes in O_2 concentrations (WTW Multimeter 350i) in the water column in the light and the dark (Staehr et al. 2012), sealing off the oxygen exchange to the atmosphere during measurements by laying a piece of plastic bubble wrap on the water surface. Gross ecosystem production (GEP) was calculated as the change in O_2 concentrations over 2-3 h during the light and respiration (R) was calculated as the change of O_2 over 2-3 h in the dark. All measurements were standardised to mg O_2/L/h and net ecosystem production (NEP) was calculated as GEP – R. Positive values of R were set to zero.

At six different time points throughout the experiment, 50 - 60 mL water was sampled for the following analyses. Pelagic primary and bacterial production (TPP, BAC) were measured using the ^{14}C uptake method, modified from Strickland and Parsons (1968); a known amount of radiolabelled carbon ($NaH^{14}CO_3$) was added to duplicate 10 ml water samples from each microcosm. One was incubated in the light and one in the dark for c. 2 h, after which all biological processes were stopped by the addition of 0.5 ml 10% HCl. Excess ^{14}C was then bubbled off, 10ml of Ultima Gold scintillation cocktail added, and ^{14}C activity in the samples measured using liquid scintillation (Tri Carb, 2910 TR, Perkin Elmer). Measurements were standardised to Bq/h/10 ml. Bacterial production is assumed to be the ^{14}C uptake during the dark and primary production is the light measurement minus the dark measurement.
After each sampling, fresh media was added to compensate for the samples taken as well as accounting for evaporation. Once a week, the amount of phytoplankton left in the microcosms was established by measuring fluorescence (see 2.1, Fig S1) and fresh *R. subcapitata* and *E. magnus* was added to ensure that 0.5 mg C/L were available for *D. magna.* The amount was increased to 1.0 mg C/L after ten days to account for *D. magna* population growth.

Additionally, the growth of *L. minor* was measured by taking photographs at six time points during the experiment, from which the number of fronds were determined using ImageJ (Rueden, et al. 2017).

2.5 Final microcosm sampling

2.5.1 Grazing and carbon assimilation rates

At the end of the experiment, 8-11 *D. magna* and three of the adult *L. peregra* were collected from each microcosm for the following assays.

Daphnia magna carbon assimilation was measured following Nascimento et al (2015). The pooled *D. magna* were placed in 50 ml Falcon tubes containing a known amount of *R. subcapitata* that had previously been labelled with ^{14}C by allowing it to grow in media spiked with $NaH^{14}CO_3$. *Daphnia* were allowed to graze for 24 h, after which they were transferred into clean media to defaecate. After preservation in ethanol, each *D. magna* was photographed to determine its length. The individuals from each replicate were pooled and dissolved in 1 ml Soluene for 48 h, after which 10 ml Ultima Gold was added and ^{14}C content was measured using liquid scintillation (Tri Carb, 2910 TR, Perkin Elmer).

To determine *L. peregra* grazing rates, we followed the methods of Crichton, et al. (2004). In short, 7.5 gFW of spinach were filtered on to a 47 mm diameter circle of GF/C filter paper, dried, weighed and then put into a small Petri dish containing artificial medium, before the snails were allowed to graze on the spinach mat (one mat / one snail) for c. 24 h. The filters were then dried and re-weighed and changes in weight calculated.

2.5.2 Primary producers

The shoots of *E. densa* and *L. nummularia* were blotted dry, weighed and photographed. *Lemna minor* was first photographed, and then collected for analysis of photosynthetic parameter and thiobarbituric acid reactive substances (TBAR) (see 2.5.4).

Photosynthetic parameters of the three plants were detected using a Pulse-Amplitude-Modulated chlorophyll fluorometer (PAM 2000; Walz, Germany). Before measurements, individual leaves of each of the plants were maintained in darkness for 30 min at room temperature (c. 20 °C). After dark adaption, the light-emitting diode was placed 3 mm above the leaf's surface. Initial fluorescence (Fo) was measured under a continually weak modulated illumination (1 µmol m^{-2} s^{-1}). Then the maximal fluorescence (Fm) was obtained by applying a 1 s single saturating flash of 5000 µmol PAR m^{-2} s^{-1} intensity. The maximum quantum efficiency of PS II primary photochemistry (ΦPSII) was estimated by the equation Fv/Fm=Fm-Fo/Fm. After decline the photosynthetic capacity (maximal quantum yield), the minimal and maximal fluorescence yield of the illuminated sample (Ft and Fm') was measured after 30 mins of continuous illumination (80 µmol PAR m^{-2} s^{-1}). In addition, saturating actinic light pulses were given to determine the photosynthetic electron transport rate (ETR) and photochemical quenching coefficients (qP and qN) (Roháček 2002).

Due to the addition of snails and plants that did not stem from sterile laboratory cultures, other phytoplankton species were also detected; these were identified to the lowest possible taxonomic level, using an inverted microscope (Table S1).

2.5.3 Consumers

Daphnia magna population size was determined through stereomicroscopic counts and photographs of Lugol-preserved specimens. From each microcosm, the size of forty randomly selected individuals were measured from photographs using ImageJ (Rueden et al. 2017).

The adults of *L. peregra* were weighed before and after the experiment to obtain growth rates. All juveniles and egg capsules were collected from the microcosm walls, plants and sediment surface. Within five randomly collected capsules from each microcosm, the number and size of the eggs were recorded using photographs and ImageJ (Rueden, et al. 2017).

2.5.4 Thiobarbituric acid reactive substances (TBARS)

The TBARS assay quantifies oxidative stress by measuring lipid peroxidation (LPO); damage to lipids results in the production of malondialdehyde (MDA), which reacts with thiobarbituric acid (TBA) under various stress conditions (Heath and Packer 1968). Samples (and weights) of the following species were included for TBARS analyses; *L. nummularia* (0.07 – 0.34 g), *E. densa* (0.08 – 0.28 g), *L. minor* (0.01 – 0.04 g), *D. magna* (0.01 – 0.14 g) and of *L. peregra* (0.01- 0.03 g). The frozen samples were homogenised using 0.5 ml of trichloroacetic acid (TCA), followed by centrifuging at 13 000 rpm for 10 min at 4 °C. The resulting 400 µl of supernatant was mixed with 1 ml of TCA-TBA reagent (20 % containing 0.5 % TCA) and kept in a block heater at 80 ° C for 30 min. After the incubation, the samples were cooled down quickly in an ice bath and centrifuged again at 13 500 g at 4 °C for 5 min. The remaining 200 µl of the supernatant were transferred into a 96 well plate with three technical replicates, and the absorption of the supernatants was measured at 532 and 600 nm in a microplate reader (Hidex Sense), at 25 °C. From these absorptions, MDA concentrations were calculated (see Supplementary Information for details).

2.6 Statistical analyses

To explore the relationship between average dose rate and the different endpoints measured (see Table 2), we used either linear or curvilinear (quadratic) regressions. The function that minimized the Akaike Information Criterion (AIC) as well as being the significantly better fit (based on ANOVA model comparisons) was chosen. Response variables were checked for normality and homogeneity of variance and model validations for all final functions were performed according to (Zuur, et al. 2009). If necessary, response variables were logarithmically transformed to improve normality.

When plants are exposed to gamma radiation, ROS may form, which may lead to structural damage in polyunsaturated lipids forming MDA or changes in the activity of the photosynthetic apparatus, which in turn can affect plant growth. We investigated these direct and indirect effects of gamma radiation on plant growth (Fig.1) using piecewise structural equation modelling (SEM). Based on previous system knowledge of causal links between variables and observed data, SEM can partition net relationships into direct and indirect effects of predictors (Grace, et al. 2010). Piecewise SEM is an extension of SEM that overcomes some of the restrictions of classical SEM models, for instance, by accounting for non-independence of data by including random variation (Lefcheck 2016). Where the curvilinear (quadratic) regressions were found to be the better fitting function, these non-linear relationships were included in the piecewise SEM. To represent the quadratic relationship between the predictor and response variable, a product variable ($predictor^2$) was created and included into the multiple regression alongside the predictor and response variable (Kline 1998). The presence of the product variable adds a "bend" to the regression line, where the regression coefficient estimates the magnitude of the quadratic aspect of the relation between predictor and response variable (Kline 1998). An additional piecewise SEM was performed to investigate whether ecological processes influenced the microcosm ecosystems regardless of dose rate. The model tested the potential direct and indirect effects of *L. minor*, *L. nummularia*, and *D. magna* on chlorophyll *a*, a proxy for total plankton biomass. SEM models were fitted with the PiecewiseSEM R package (Lefcheck 2016). The overall fit of the models were evaluated using Shipley's test of d-separation. Fisher's C statistic was used to test for missing paths; $p > 0.05$ indicates that the model fits the data well and there are no missing paths. Different models were compared based on AIC values adjusted for small sample size (AICc).

Additionally, principle component analyses (PCA) were performed to investigate the relative importance of ecosystem processes (NEP, R, TPP, BAC; see 2.4) over time. We applied an unconstrained redundancy analysis (Fritsch, et al.) to the NEP and R data as well as the TPP and BAC data using the Vegan R package (Oksanen, et al. 2016).

All statistical analyses were performed in R version 3.3.3 (Team 2017). The significance levels were set to $\alpha = 0.05$.

3. Results

In general, external gamma radiation had a stronger effect on the primary producers than on the consumers in the microcosms. Water temperature (18.7 °C ± 0.41 SD), pH (7.2 ± 0.13 SD), conductivity (179.7 µs/cm ± 37.5 SD µs/cm) and light (1192.3 lux ± 119.1 SD) were relatively stable throughout the experiment (Supplementary Information, Table S2).

3.1 Primary producers

While no effect of dose rate was found on *L. nummularia* and *E. densa* growth rates (Fig. 4 a), the biomass of both plants was higher at the end of the experiment, with growth rates varying from 72 to 203 mg FW/day and 42 to 198 mg FW/day, respectively. *L. minor* population growth rates decreased significantly with increasing average dose rate (Fig. 4 b).

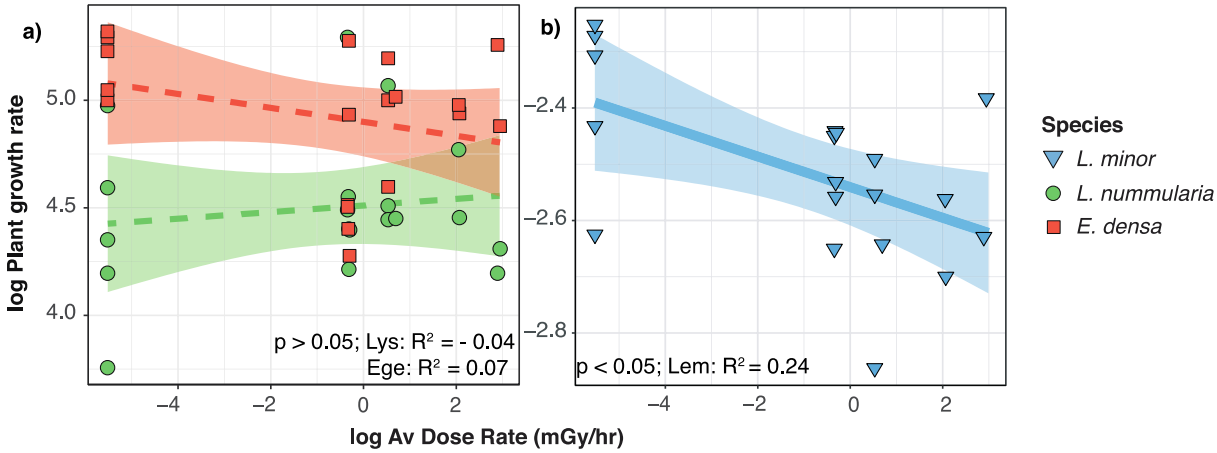

Fig. 4. Growth rates of a) L. nummularia and E. densa as increase of biomass over time (mgFW/day), and b) L. minor as population growth per day, predicted by average dose rate (mGy h^{-1}). Dashed lines indicate non-significant relationships while solid lines indicate significant relationships. P-values and adjusted R^2 are displayed.

The photosynthetic responses of *L. minor*, *L. nummularia* and *E. densa* were negatively affected by increasing average dose rate. The maximal efficiency of PS II (ΦPSII) significantly decreased in all three macrophytes (Fig. 5; II a-c) and the electron transport rate (ETR) was also significantly inhibited (Fig. 5; I a-c). There was a significant decrease of photochemical quenching (qP, Fig. 5; III a-c), while non-photochemical quenching or heat production increased significantly with increasing average dose rate (qN, Fig. 5; IV a-c).

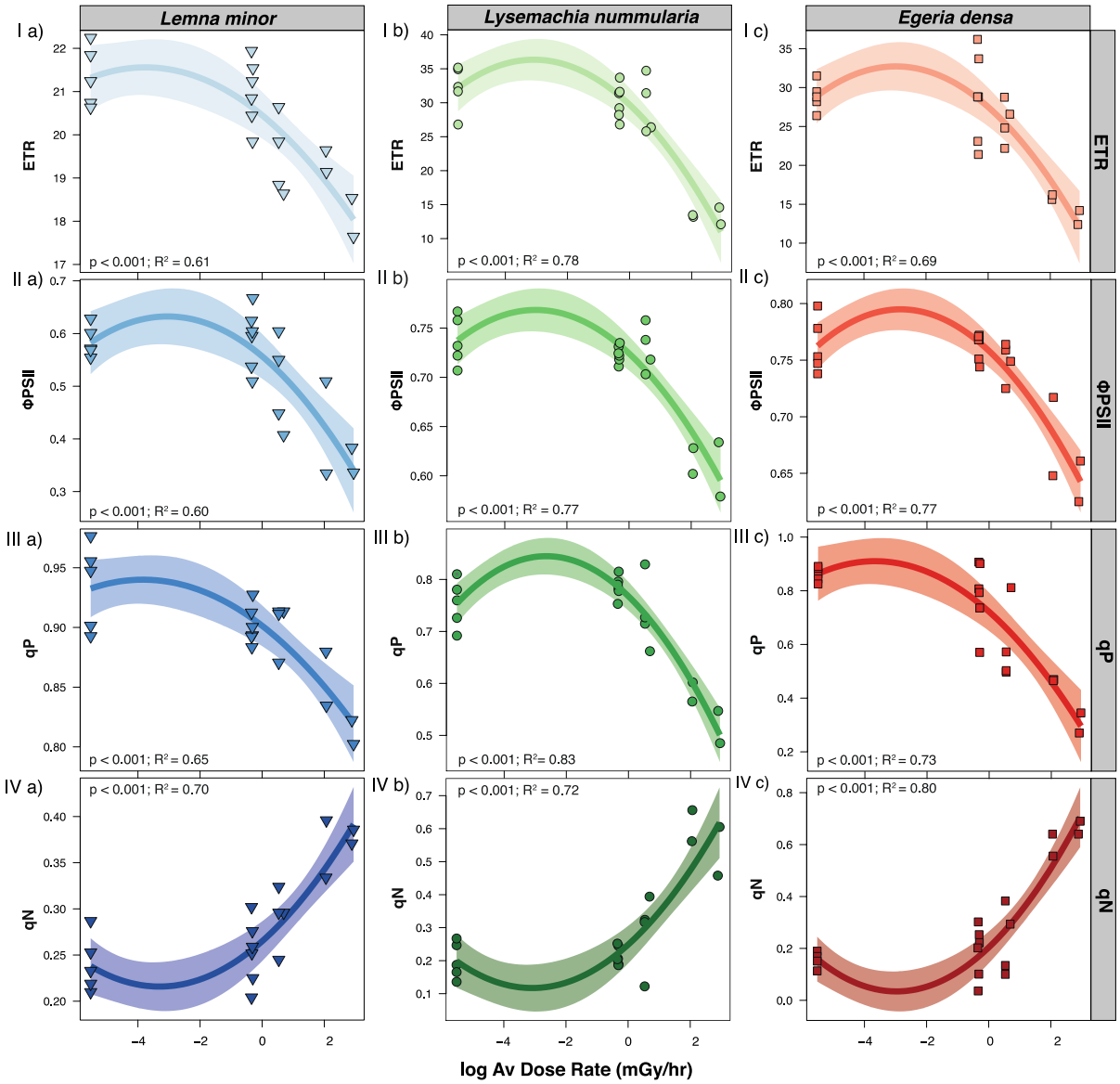

Figure 5. Response of chlorophyll fluorescence emission measurements to increasing average dose rate (mGy h^{-1}) in a) L. minor, b) L. nummularia and c) E. densa. I) ETR, II) ΦPS II, and photochemical quenching coefficients III) qP and IV) qN. P-values and adjusted R^2 are displayed.

Piecewise SEM models on the effects of dose rate and MDA concentrations on *L. minor*, *L. nummularia* and *E. densa* growth rates fitted the data well (Fisher's C = 2.31, 2.92 and 0.01, and *P* = 0.31, 0.23 and 0.99, respectively). In the model for *L. minor*, average dose rate had a negative effect on both growth rate and ETR, however no indirect effects of dose rate on growth rate were observed (Fig. 6 a). For *L. nummularia*, the only significant effect was a direct negative effect of average dose rate on ETR (Fig. 6 b), while in the model for *E. densa* average dose rate had a direct negative effect and an indirect (through ETR) positive effect on growth rate (Fig. 6 c). However, in this case overall effect of average dose rate on *E. densa* could be calculated; it was negative (-0.18), as the positive indirect effect (0.06) was rather small (MacKinnon, et al. 1995).

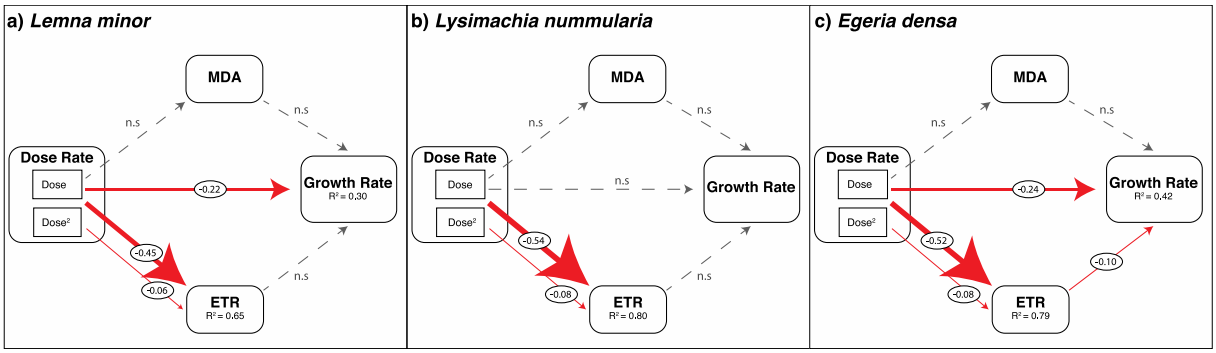

Figure 6. Piecewise structural equation 13odelling (SEM) of logarithmically transformed average dose rate, MDA (nmol / wet weight (g)) and ETR as predictors of a) L. minor, b) L. nummularia and c) E. densa growth rates. For the effect of dose rate on ETR a product variable Dose² has been included to account for the quadratic relationship. Path coefficients are reported as standardized effect size. Solid red arrows represent significant negative paths (p < 0.05) and are scaled based on standardized coefficients. Dashed grey lines represent non-significant paths.

The model exploring ecological processes regardless of dose rate also fitted the data well, with a Fisher's C = 1.77 and P = 0.412. *L. minor* growth had a direct negative effect on *L. nummularia* growth, and pelagic chlorophyll *a* concentrations (phytoplankton biomass) decreased in all treatments during the course of the experiment (Fig S1) and were negatively influenced by *D. magna* abundance (Fig. 7). However, none of the potential indirect effects were significant.

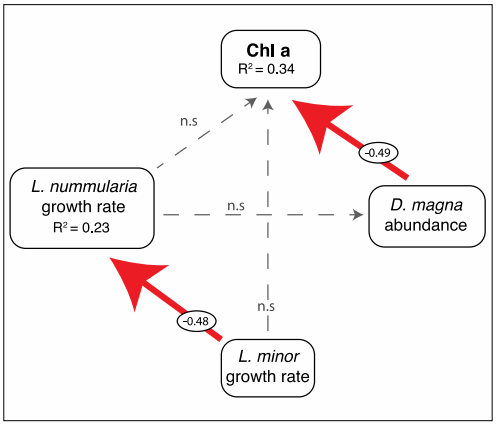

Figure 7. Piecewise structural equation modeling (SEM) of L. minor growth as predictor of L. nummularia growth, D. magna and pelagic chlorophyll a (phytoplankton biomass), which was also predicted by D. magna abundance. Path coefficients are reported as standardized effect size. Solid red arrows represent significant negative paths (p < 0.05) and are scaled based on standardized coefficients. Dashed grey arrows non-significant paths.

3. 2 Primary consumers

All *L. peregra* individuals added at the start of the experiment survived the duration of the experiment and reproduced more than once during the experiment in all microcosms. Reproduction cycles were evident by the appearance of juveniles around week 2 and new egg capsules at week 3. There was some evidence of decreased number of juveniles and number of eggs with increasing average dose rate (Table 2); however, low sampling number at high doses resulted in insufficient statistical power to support these trends. There was no significant effect of dose rate on *L. peregra* grazing rates (Table 2).

Table 2. List of all endpoints measured and their response to radiation. Dose response relationships were statistically tested using regression analyses.

	Endpoints Measured	**Affected by radiation**
Ecosystem Endpoints		
	NPP	No
	R	No
	GPP	No
	Total Primary Production	No
	Bacterial Production	No
Ecological Endpoints		
	L. peregra grazing rates	No
	D. magna carbon incorporation	No
	Chlorophyll *a*	No
Individual species endpoints		
	L. minor growth	Yes (see Fig 4)
	L. minor ETR	Yes (see Fig 5)
	L. minor ΦPSII	Yes (see Fig 5)
	L. minor qP	Yes (see Fig 5)
	L. minor qN	Yes (see Fig 5)
	L. minor MDA	No
	L. nummularia growth	No (see Fig 4)
	L. nummularia ETR	Yes (see Fig 5)
	L. nummularia ΦPSII	Yes (see Fig 5)
	L. nummularia qP	Yes (see Fig 5)
	L. nummularia qN	Yes (see Fig 5)
	L. nummularia MDA	No
	E. densa growth	Not directly (see Fig 4 & Fig 5)
	E. densa ETR	Yes (see Fig 5)
	E. densa ΦPSII	Yes (see Fig 5)
	E. densa qP	Yes (see Fig 5)
	E. densa qN	Yes (see Fig 5)
	E. densa MDA	No
	L. peregra growth	No
	L. peregra egg capsual production	No
	L. peregra number per egg capsual	No
	L. peregra number juveniles	No
	L. peregra MDA	No
	D. magna length	No
	D. magna abundance	No
	D. magna MDA	No
	Leaf litter loss	No

Daphnia magna abundance showed a significant increase over the course of the experiment, starting at 12 individuals per microcosm and reaching population sizes in the range from 160 to 400 individuals. However, there were no significant differences between the dose rates (Table 2). There was also no significant effect of dose rate on *D. magna* carbon assimilation (Table 2).

3.3 Whole ecosystem endpoints

Net ecosystem productivity (NEP) decreased over time across all dose rates. This decrease was most pronounced for periods between T0 (1.59 ± 0.05 mg C/L/h) to T4

(0.12 ± 0.08 mg C/L/h), thereafter remaining low across all dose rates. This is also evident from the PCA for NEP and R (Fig. 8a), where PC1 explained 73.6 % and PC2 26.5% of the variability. The spread within each time point seems to be due to variation in respiration, while the difference between T0 and the last two time points seems to be caused by a decrease in NEP. No significant effects of dose rates were observed.

Pelagic primary and bacterial production (TPP, BAC) decreased from T0 and T4 to T22, and there were no significant differences between dose rates. The PCA shows a slight shift from T0 and T4 while T22 is distinctly different (Fig. 8b). PC1 explained 85.5 % and PC2 11.5% of the variability.

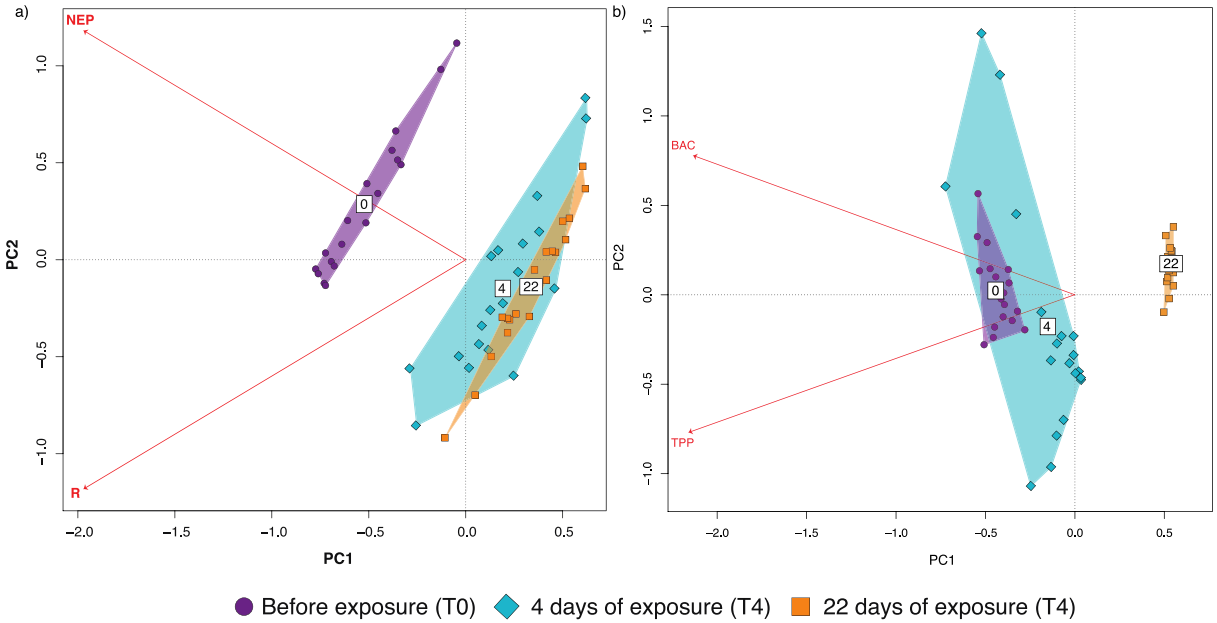

Figure 8. Biplots of a) PCA based on net ecosystem production (NEP) and respiration (R), and b) PCA based on total pelagic primary production (TPP) and bacterial production. Each symbol represents one microcosm at each time point. The centroids are time points T0 (0), T4 (4) and T22 (22), also indicated by colour of symbols and shaded areas.

4. Discussion

This study investigated the effects of external gamma irradiation and ecological processes on an experimental aquatic ecosystem. A large range of endpoints, from molecular- to ecosystem-level, were measured in order to try and capture potential direct and indirect effects of radiation. This experiment is the first microcosm study, to our knowledge, to have used experimental dose rates similar to those experienced by organisms in the field during the acute and intermediate phases of a nuclear accident. The clearest radiation effects were seen in the primary producers and at molecular rather than individual or population level. Effects on species interactions and indirect effects were harder to determine. This could be due to the natural variability between microcosms, the insufficient duration of the experiment and possibly buffering effects within the ecosystem. Below we discuss our results in the context of other single-species irradiation experiments. We also suggest a number of recommendations for future microcosm studies with radiation, which we believe can fill a methodological gap in radioecology in the future.

4.1Primary producers

Photosynthetic parameters, such as øPSII, ETR, qP and qN, are a direct measure of a plant's ability to convert light energy to chemical energy, which is essential for plant growth and, ultimately, survival. The reduction of øPSII, ETR and qP seen across all three macrophytes could be a stress response induced by gamma radiation, since changes in photosynthetic parameters have been used as indicators of toxicity (Juneau, et al. 2002; 2005). Gamma radiation induces reactive oxygen species (ROS) that can trigger the degradation of the D1 protein and reduced reparation in PS II (Nishiyama, et al. 2001), which will cause PS II inhibition and block energy pathways (electron transport chain) in the thylakoid membranes. Energy can therefore not be used for ATP synthesis in the chloroplasts resulting in increased non-photochemical quenching (qN) to convert the excess energy to heat (Carbonara, et al. 2012), a common photo-protective mechanism (Juneau et al. 2005). Responses in photosynthetic parameters in *L. minor* were seen at much lower dose rates than earlier results from Van Hoeck, et al. (2017) whose lowest dose rate was 25 mGy h^{-1} (for 7 days). Interestingly, those authors observed the opposite trend to our study, with increased photosynthetic capacity (light-saturated maximum photosynthesis (A_{max}) in exposed *L. minor*. In combination with data on up- and down-regulation of relevant genes, they interpreted this as an acclimation response.

It is difficult to compare results from different studies since plant species, organelles and developmental stage influence the extent of the radiation-induced effects (Van Hoeck, et al. 2015). However, the apparent higher sensitivity of the *L. minor* in our experiments compared to previous studies may be due to a number of factors. In single species tests, conditions (e.g. light, pH, nutrients) are optimised for the study species, whereas in a multispecies experiment (as in the field), conditions are often suboptimal for any one species but maintain the community as a whole. For example, in this experiment a light intensity of c. 1200 lux was used, compared to 6500-10000 lux recommended for standard *L. minor* ecotoxicology tests (OECD 2006), and nutrient concentrations were at the lower end of the recommended range. In the microcosms, *L. minor* would also have been competing for nutrients with the other two plant species and phytoplankton and subjected to snails grazing on their leaves and roots (pers. obs.). Piecewise SEM analysis (Fig. 7) seems to support this hypothesis, showing a negative relationship between *L. minor* growth and *L. nummularia* growth, suggesting competition.

Although radiation affected all three plants' photosynthetic capabilities, no membrane damage (as measured by the lipid peroxidation product MDA) was observed, and all three species continued to grow throughout the experiment. However, the growth rates of both *L. minor* (Fig. 4b, 6a) and *E. densa* (Fig. 4a, 6c) were suppressed. It is interesting to note that a simple linear regression revealed no significant effect of dose rate on *E. densa* growth (Fig. 4a), whereas this relationship was significant in the SEM analysis, where the influence of multiple factors was considered simultaneously and radiation shown to contribute to the overall effects (Fig. 6c). This supports the argument that we may not be able to identify the effects of the stressor of interest by examining single endpoints or species separately, but these may be identified if other factors are taken into account. The SEM also revealed that a significantly decreased ETR directly affected growth rate in *E. densa*, a result we might expect across all plant species if the experiment had continued beyond 22 days. It is possible that *E. densa* is more radiosensitive than *L. minor* and *L. nummularia*.

The other primary producers in the microcosms were phytoplankton, whose population diminished quickly, contributing to less primary production across all dose rates, including controls (Fig. 8). The lack of differences in phytoplankton biomass and productivity between treatments is perhaps not surprising given that phytoplankton were added periodically throughout the experiment. In addition,

previous authors have only seen phytoplankton responses at much higher dose rates or doses (100 Gy acute dose - Fuma et al. 2010; 9.7 Gy d^{-1} for 305 d - Fuma et al. 2012; >50 Gy at 6.7 Gy min^{-1} - Nascimento and Bradshaw 2016). Piecewise SEM was used to investigate the potential influence of two ecological processes on the phytoplankton population - i) competition for nutrients with the macrophytes *L. nummularia* and *L. minor* and ii) grazing by *D. magna* (Fig. 7) - and indicated that *D. magna* abundance was the dominating factor controlling phytoplankton biomass.

Daphnia magna was insensitive to radiation in this experiment; all populations increased c. 15-fold during the experiment and there were no effects of dose rate on MDA concentrations, carbon assimilation, individual size or population size. This is in line with Gilbin, et al. (2008) who saw no effects on *D. magna* survival or grazing rates at dose rates up to 31 mGy h^{-1} (over 23 days), and Nascimento and Bradshaw (2016) who saw little effect on grazing rates or individual size below 273 mGy h^{-1} (for 3 days). However, Gilbin et al. (2008) observed a 21% decrease in individual fecundity after 23 days at 31 mGy h-1 and Parisot et al. (2015) found increased juvenile mortality and delayed reproduction in the F1 and F2 generations at a similar external gamma dose rate range to ours.

There were no significant effects of radiation on *L. peregra*. However, snail grazing rates showed a decreasing, though non-significant, trend with increasing dose rate, as did their reproductive capacity (eggs per capsule and number of juveniles; Table 2). Cooley and Miller (1971) exposed freshwater snails *Physa heterostropha* to gamma radiation and also saw indications of lower egg production at similar dose levels to ours (1 rad h^{-1} (= 10 mGy h^{-1}) for 4 months), and significantly reduced life span, growth and egg production at 10 rad h^{-1} (100 mGy h^{-1}). The authors argue that the snails in their experiment were quite radiosensitive, especially regarding reproduction.

4.3 Ecosystem processes

The change in ecosystem functions, particularly production, from the start to the end of the experiment (Fig. 8 a and b) across all dose rates is likely due to stabilisation of the systems over time. NEP may have been high at the start (T0) since the macrophytes were establishing themselves, e.g., by growing roots. In addition, there was a large decrease in phytoplankton abundance during the first week due to rapidly increasing *D. magna* populations. *Daphnia* blooms during the first 15-30 days have been typical in microcosm studies (Taub, 1984, 1997; Meador et al. 1993) and are often followed by nutrient depletion, decreased net primary productivity, reduction of *Daphnia* populations and thereafter a period of equilibrium.

The significant shifts in NEP from T0 to T4 in our experiment could thus be due to sampling the microcosms before the systems had fully stabilised. The first measurements (T0) were taken after 3 days of stabilisation, and Taub et al. (1984) reported that although no long pre-treatment period is necessary, at 7 days (i.e., T4 in our experiment) the communities are likely well synchronised. The microcosms in our study appear to support this theory, since NEP and R change little from T4 to T22. A balance between production and respiration reflects a balanced ecosystem (Giesy, 1980; Odum, 1985).

Direct comparisons of respiration and production with other published data are difficult, since they are functions of biomass, light and nutrient levels (Abbott, 1966). However, reduced productivity (NEP and TPP) after T4, such as we measured by both low O_2 production and ^{14}C incorporation, has also been measured as an indication of inhibited photosynthesis due to stress (Kobraei and White 1996). Although we saw evidence of photosynthetic stress in all three plant species (see 4.1), this was dose-rate dependent and cannot explain the overall decrease and continued low NEP at all dose rates. All plant species continued to grow throughout the experiment and did not show extensive evidence of grazing by *L. peregra*. There may

therefore have been a relative stabilisation after T4 in the balance between NEP (O_2 produced from increasing biomass of plants and possibly biofilm) and R (O_2 consumed by the primary producers but also by increasing numbers of *L. peregra*, *D. magna* and probably benthic and pelagic bacteria). Bacteria certainly came to dominate the pelagic part of the ecosystem by the end of the experiment; pelagic bacterial production decreased more slowly than pelagic primary production (TPP) and was approximately seven times higher than TPP by T22. In addition, benthic bacteria were active in all cosms, as indicated by a loss of leaf litter dry biomass over the experimental period.

4.4 Species interactions, indirect and ecosystem effects

This study set out to characterise and quantify species interactions and indirect effects, since they may be as important as direct effects of contaminants and mediate overall ecosystem responses to stress (Preston et al. 2002, Fleeger et al. 2003). Species interactions were measured directly (*D. magna* carbon assimilation and *L. peregra* grazing rates) and indirect effects were quantified and analysed through path analyses (SEM). No significant effects of radiation were observed on either species interactions or indirect effects at the dose rates and time scale of this experiment, though some dose-dependent trends were seen. However, these processes and interactions were essential in determining the ecosystem structure and function in a way that was unrelated to dose rate. The most obvious example was that *D. magna* abundance and carbon assimilation were unaffected by radiation but *D. magna* abundance (which varied between microcosms for reasons unrelated to radiation) strongly negatively affected chlorophyll a abundance (Fig. 7). In addition, *L. peregra* grazing rates showed a decreasing, though non-significant, trend with increasing dose rate, and this species is known to feed on microalgae (Vermaat et al. 1994), which might be another reason for the rapid decline of phytoplankton in our microcosms. *E. magnus*, one of the phytoplankton taxa included in this study, tends to settle out quickly onto the sediment (pers. obs.), where it could have been grazed by the snail populations. Over longer time scales, the relative sensitivities of grazers and their food species will determine whether grazers will ultimately become food limited or their food species will be released from grazing pressure (Fleeger, et al. 2003).

While *L. minor* was more sensitive to radiation than in previous single species studies using the same or similar dose rates (4.1), *D. magna* seemed to be less sensitive (4.2). In addition, we observed a significant stress response of plants at the molecular level that was not so apparent at individual or population level. It is possible that the stress reactions of organisms in the microcosms were alleviated by the surrounding microcosm's "buffering capacity" (Elmqvist et al. 2003, Fester et al. 2015). We argue that in some cases, when species are exposed to radiation in single species tests they are without a buffering capacity which can make them more sensitive. This idea of buffering capacity corresponds to Polikarpov (1998)'s "zone of ecological masking", ranging 0.006 – 0.46 mGy h^{-1}, which is at the low end of our exposure range.

4.5 Recommendations for future radioecological microcosm studies

The pros and cons of cosm studies have already been addressed by numerous authors (Benton, et al. 2007; Beyers and Odum 1993; Drake and Kramer 2012; Giesy 1980). Microcosms are by necessity and design a compromise between a true representation of natural environments and a controlled experimental system with reduced complexity at the expense of realism (Beyers and Odum 1993). Many decisions must be taken when setting up a microcosm experiment and guidelines have been published (Giesy Jr and Odum 1980; Taub 1989). Examples from these include whether additional nutrients or food should be added during the experiment

to mimic inflow from the surrounding environment and sustain the systems (as in this experiment), or whether the microcosms should be self-sustaining, something that is notoriously difficult to achieve over long periods of time. Ultimately, the experimental design can vary greatly among microcosm studies depending on the research question of interest, examples can be found in several reviews of microcosm studies (Giesy JR 1980; Lasserre 1990; Van den Brink et al 2005).

Regardless of design, small initial differences between replicates may increase with time. Stochastic events may also lead to differences between replicates. Such variability can make interpretation of the data difficult and should, if possible, be minimized. For this reason, most microcosm studies (including this one) standardise the initial numbers and/or biomass of the different compartments. To further standardise starting conditions, microcosm studies can also aim to ensure that the lifecycles of each compartment of the system are as synchronised as possible. In our case daphniid populations could have been counted at the start of the exposure (and not only when they were initially added), and the number of gravid females standardised between replicates.

The length of time that a microcosm study is run depends on several factors, and for radiation studies the availability of facilities may be a limiting factor. However, for chronic exposures, ideally the duration should cover a few generations of the majority of the included organisms. In this study, we believe that a longer experimental duration may have allowed further effects to be manifested. In previous multigenerational studies with *D. magna* at external gamma exposures in a similar dose rate range to ours, the F1 and F2 generations showed increased juvenile mortality and delayed reproduction (Parisot et al. 2015). Given the number of daphniids present at the end of our experiment (160-400 individuals), the 22 day timespan of the microcosm study was probably just sufficient for the first F2 individuals to start appearing; with a longer experimental duration we would expect that reproduction and growth effects would have started to be manifested, at least at the higher dose levels. Similarly, for the snail *L. peregra,* that reproduces continuously (Wullschleger and Jokela 2002) for most of its life span from c. 7 and up to 30 weeks, we estimate from observations of the numbers and sizes of juveniles that the adult snails had reproduced about twice by the end of the exposure. Given the decreasing trends in grazing rates and reproductive capacity (eggs per capsule and number of juveniles) with increased dose, a longer exposure could have resulted in a dose-dependent population reduction. With time, a reduced snail population and decreased per capita grazing rate could have an important effect on the ecosystem since they are the main organisms grazing down the biofilm.

The few irradiation exposure facilities that exist for radioecological studies are generally based on a similar design – a radiation point source producing a radiation field that is strongest closest to the source and weakest furthest away. Thus, the geometry of the radiation field always means that there will be less space for the higher dose treatments, and thus less possibility for extensive replication. However, higher dose treatments are important since, even if they are not so environmentally relevant, they enable a larger radiation gradient (i.e., more of the dose response curve) to be investigated, which is essential for drawing wider conclusions about radiation effects.

This is the first radioecological effects study to be done with microcosms at these dose rates (previous aquatic microcosm studies have been mainly with microbial and/or planktonic organisms and dose rates orders of magnitude higher than ours). More radioecology microcosm studies are needed in order to build up a larger knowledge base on the ranges of dose rates where effects of radiation on species interactions and community- and ecosystem-level endpoints can be measured.

5. Acknowledgements

We are grateful to the Nordic Nuclear Safety Research (NKS) for financial support of this project. This work is also supported by the Research Council of Norway through its Centres of Excellence funding scheme, project number 223268/F50 (received through the Centre for Environmental Radioactivity, CERAD).

We wish to thank L. Rossbach, I. Holmerin, D. Oughton, L. Kiel Jensen, T. Tuovinen and Dag Anders Brede for the assistance and support throughout the experiment, and N. Stjärnkvist and E. El-Marhoumi for assistance during sample analysis.

We thank three anonymous reviewers and the Editor for comments, which greatly improved the paper.

6. References

Abbott W 1966. Microcosm studies on estuarine waters I. The replicability of microcosms. Journal (Water Pollution Control Federation): 258-270.

Agostinelli S, Allison J, Amako K, Apostolakis J, Araujo H, Arce P, Asai M, Axen D, Banerjee S, Barrand G, al. e 2003. Geant4—a simulation toolkit. Nuclear Instruments and Methods in Physics Research Section A: Accelerators, Spectrometers, Detectors and Associated Equipment 506: 250-303. doi: https://doi.org/10.1016/S0168-9002(03)01368-8

Alexakhin R, Karaban R, Prister B, Spirin D, Romanov G, Mishenkov N, Spiridonov S, Fesenko S, Fyodorov YA, Tikhomirov F 1994. The effects of acute irradiation on a forest biogeocenosis; experimental data, model and practical applications for accidental cases. Science of the Total Environment 157: 357-369.

Allison J, Amako K, Apostolakis J, Arce P, Asai M, Aso T, Bagli E, Bagulya A, Banerjee S, Barrand G, al. e 2006. Geant4 developments and applications. IEEE Transactions on Nuclear Science 53: 270-278. doi: 10.1109/TNS.2006.869826

Allison J, Amako K, Apostolakis J, Arce P, Asai M, Aso T, Bagli E, Bagulya A, Banerjee S, Barrand G, Beck BR, al. e 2016. Recent developments in Geant4. Nuclear Instruments and Methods in Physics Research Section A: Accelerators, Spectrometers, Detectors and Associated Equipment 835: 186-225. doi: https://doi.org/10.1016/j.nima.2016.06.125

Alonzo F, Gilbin R, Bourrachot S, Floriani M, Morello M, Garnier-Laplace J 2006. Effects of chronic internal alpha irradiation on physiology, growth and reproductive success of Daphnia magna. Aquatic toxicology 80: 228-236.

Alonzo F, Gilbin R, Zeman F, Garnier-Laplace J 2008. Increased effects of internal alpha irradiation in Daphnia magna after chronic exposure over three successive generations. Aquatic toxicology 87: 146-156.

Amiro B, Sheppard S 1994. Effects of ionizing radiation on the boreal forest: Canada's FIG experiment, with implications for radionuclides. Science of the Total Environment 157: 371-382.

Beketov MA, Liess M 2012. Ecotoxicology and macroecology–time for integration. Environmental Pollution 162: 247-254.

Benton TG, Solan M, Travis JM, Sait SM 2007. Microcosm experiments can inform global ecological problems. Trends in Ecology & Evolution 22: 516-521.

Beyers RJ, Odum HT. 1993. Ecological microcosms: Springer-Verlag.

Bjerke H, Hetland PO. 2014. The gamma irradiation facility FIGARO – Report on the measurements of dose rate in the cobolt-60 irradiation field. Technical Document. 2. In.

Bradshaw C, Kapustka L, Barnthouse L, Brown J, Ciffroy P, Forbes V, Geras' kin S, Kautsky U, Bréchignac F 2014. Using an ecosystem approach to complement protection schemes based on organism-level endpoints. Journal of environmental radioactivity 136: 98-104.

Brechignac F 2003. Protection of the environment: how to position radioprotection in an ecological risk assessment perspective. Science of the Total Environment 307: 35-54.

Bréchignac F, Bradshaw C, Carroll S, Fuma S, Håkanson L, Jaworska A, Kapustka L, Kawaguchi I, Monte L, Oughton D 2012. Towards an ecosystem approach for environment protection with emphasis on radiological hazards. IUR, Report 7.

Brèchignac F, Doi M 2009. Challenging the current strategy of radiological protection of the environment: arguments for an ecosystem approach. Journal of environmental radioactivity 100: 1125-1134.
Bréchignac F, Oughton D, Mays C, Barnthouse L, Beasley JC, Bonisoli-Alquati A, Bradshaw C, Brown J, Dray S, Geras' kin S 2016. Addressing ecological effects of radiation on populations and ecosystems to improve protection of the environment against radiation: Agreed statements from a Consensus Symposium. Journal of environmental radioactivity 158: 21-29.
Carbonara T, Pascale R, Argentieri MP, Papadia P, Fanizzi FP, Villanova L, Avato P 2012. Phytochemical analysis of a herbal tea from Artemisia annua L. Journal of pharmaceutical and biomedical analysis 62: 79-86.
Clements WH, Kiffney PM 1994. Assessing contaminant effects at higher levels of biological organization. Environmental Toxicology and Chemistry 13: 357-359.
Cooley J 1973. Effects of chronic environmental radiation on a natural population of the aquatic snail Physa heterostropha. Radiation Research 54: 130-140.
Cooley J. 1971. Effects of temperature and chronic irradiation on populations of the aquatic snail Physa heterostropha. In.
Cooley J, Miller Jr F 1971. Effects of chronic irradiation on laboratory populations of the aquatic snail Physa heterostropha. Radiation Research 47: 716-724.
Copplestone D, Hingston J, Real A 2008. The development and purpose of the FREDERICA radiation effects database. Journal of environmental radioactivity 99: 1456-1463.
Crichton C, Conrad A, Baird D 2004. Assessing stream grazer response to stress: a post-exposure feeding bioassay using the freshwater snail Lymnaea peregra (Müller). Bulletin of environmental contamination and toxicology 72: 564-570.
Dallas LJ, Keith-Roach M, Lyons BP, Jha AN 2012. Assessing the impact of ionizing radiation on aquatic invertebrates: a critical review. Radiation Research 177: 693-716.
Drake JM, Kramer AM 2012. Mechanistic analogy: how microcosms explain nature. Theoretical ecology 5: 433-444.
Ferens MC, Beyers RJ 1972. Studies of a simple laboratory microecosystem: effects of stress. Ecology 53: 709-713.
Fleeger JW, Carman KR, Nisbet RM 2003. Indirect effects of contaminants in aquatic ecosystems. Science of the Total Environment 317: 207-233.
Fritsch C, Scheifler R, Beaugelin-Seiller K, Hubert P, Cœurdassier M, De Vaufleury A, Badot PM 2008. Biotic interactions modify the transfer of cesium-137 in a soil-earthworm-plant-snail food web. Environmental Toxicology and Chemistry 27: 1698-1707.
Fuma S, Ishii N, Takeda H, Doi K, Kawaguchi I, Shikano S, Tanaka N, Inamori Y 2010. Effects of acute gamma-irradiation on community structure of the aquatic microbial microcosm. Journal of environmental radioactivity 101: 915-922. doi: 10.1016/j.jenvrad.2010.06.007
Fuma S, Ishii N, Takeda H, Miyamoto K, Yanagisawa K, Doi K, Kawaguchi I, Tanaka N, Inamori Y, Polikarpov GG 2009. Effects of acute gamma-irradiation on the aquatic microbial microcosm in comparison with chemicals. Journal of environmental radioactivity 100: 1027-1033. doi: 10.1016/j.jenvrad.2009.06.007
Fuma S, Ishii N, Takeda H, Miyamoto K, Yanagisawa K, Doi K, Kawaguchi I, Tanaka N, Inamori Y, Polikarpov GG 1998. Effects of gamma-rays on the populations of the steady-state ecological microcosm. International journal of radiation biology 74: 145-150.
Fuma S, Kawaguchi I, Kubota Y, Yoshida S, Kawabata Zi, Polikarpov GG 2012. Effects of chronic gamma-irradiation on the aquatic microbial microcosm: equi-dosimetric comparison with effects of heavy metals. Journal of environmental radioactivity 104: 81-86. doi: 10.1016/j.jenvrad.2011.09.005
Garnier-Laplace J, Beaugelin-Seiller K, Hinton TG. 2011. Fukushima wildlife dose reconstruction signals ecological consequences. In: ACS Publications.
Garnier-Laplace J, Della-Vedova C, Gilbin R, Copplestone D, Hingston J, Ciffroy P 2006. First derivation of predicted-no-effect values for freshwater and terrestrial ecosystems exposed to radioactive substances. Environmental science & technology 40: 6498-6505.
Garnier-Laplace J, Geras'kin S, Della-Vedova C, Beaugelin-Seiller K, Hinton T, Real A, Oudalova A 2013. Are radiosensitivity data derived from natural field conditions consistent with data from controlled exposures? A case study of Chernobyl wildlife chronically exposed to low dose rates. Journal of environmental radioactivity 121: 12-21.

Geras' kin S, Fesenko S, Alexakhin R 2008. Effects of non-human species irradiation after the Chernobyl NPP accident. Environment International 34: 880-897.
Geras'kin S, Dikareva N, Oudalova A, Vasil'ev D, Volkova PY 2016. The consequences of chronic radiation exposure of scots pine in the remote period after the Chernobyl accident. Russian journal of ecology 47: 26-38.
Geras'kin SA 2016. Ecological effects of exposure to enhanced levels of ionizing radiation. Journal of environmental radioactivity 162: 347-357.
Giesy JP. 1980. Microcosms in ecological research. Springfield, VA,: Technical Information Center.
Giesy Jr JP, Odum EP 1980. Microcosmology: introductory comments. Microcosms in ecological research 52.
Gilbin R, Alonzo F, Garnier-Laplace J 2008. Effects of chronic external gamma irradiation on growth and reproductive success of Daphnia magna. Journal of environmental radioactivity 99: 134-145.
Gomes T, Xie L, Brede D, Lind O-C, Solhaug KA, Salbu B, Tollefsen KE 2017. Sensitivity of the green algae Chlamydomonas reinhardtii to gamma radiation: Photosynthetic performance and ROS formation. Aquatic toxicology 183: 1-10.
Grace JB, Anderson TM, Olff H, Scheiner SM 2010. On the specification of structural equation models for ecological systems. Ecological Monographs 80: 67-87.
Guillard RR, Lorenzen CJ 1972. Yellow-green algae with chlorophyllide C. Journal of Phycology 8: 10-14.
Hansen E, Lind O, Oughton D, Salbu B 2019. A framework for exposure characterization and gamma dosimetry at the NMBU FIGARO irradiation facility. International journal of radiation biology: 1-25.
Heath RL, Packer L 1968. Photoperoxidation in isolated chloroplasts: I. Kinetics and stoichiometry of fatty acid peroxidation. Archives of biochemistry and biophysics 125: 189-198.
ICRP 2007. The ICRP 2007 recommendations. Radiation protection dosimetry 127: 2-7.
IUR. 2002. Protection of the Environment. Current Status and Future Work International Union of Radioecology. In. IUR Report 03. Osteras, Norway.
Juneau P, El Berdey A, Popovic R 2002. PAM fluorometry in the determination of the sensitivity of Chlorella vulgaris, Selenastrum capricornutum, and Chlamydomonas reinhardtii to copper. Archives of environmental contamination and toxicology 42: 155-164.
Juneau P, Green B, Harrison P 2005. Simulation of Pulse-Amplitude-Modulated (PAM) fluorescence: Limitations of some PAM-parameters in studying environmental stress effects. Photosynthetica 43: 75-83.
Kline RB 1998. Software review: Software programs for structural equation modeling: Amos, EQS, and LISREL. Journal of psychoeducational assessment 16: 343-364.
Knowles J, Greenwood L 1997. A comparison of the effects of long-term β-and γ-irradiation on the reproductive performance of a marine invertebrate Ophryotrocha diadema (Polychaeta, Dorvilleidae). Journal of environmental radioactivity 34: 1-7.
Kobraei M, White D 1996. Effects of 2, 4-dichlorophenoxyacetic acid on Kentucky algae: simultaneous laboratory and field toxicity testings. Archives of environmental contamination and toxicology 31: 571-580.
Lefcheck JS 2016. piecewiseSEM: Piecewise structural equation modelling in r for ecology, evolution, and systematics. Methods in Ecology and Evolution 7: 573-579.
Lind, O.C., Helen Oughton, D., Salbu, B., 2018. The NMBU FIGARO low dose irradiation facility.International Journal of Radiation Biology, 1-6.
MacKinnon DP, Warsi G, Dwyer JH 1995. A simulation study of mediated effect measures. Multivariate behavioral research 30: 41-62.
McKenzie A 1995. Cobalt-60 gamma-ray beams. BJR supplement 25: 46-61.
Meador JP, Taub FB, Sibley TH 1993. Copper dynamics and the mechanism of ecosystem level recovery in a standardized aquatic microcosm. Ecological Applications 3: 139-155.
Nascimento FJ, Bradshaw C 2016. Direct and indirect effects of ionizing radiation on grazer–phytoplankton interactions. Journal of environmental radioactivity 155: 63-70.
Nascimento FJ, Svendsen C, Bradshaw C 2016. Joint toxicity of cadmium and ionizing radiation on zooplankton carbon incorporation, growth and mobility. Environmental science & technology 50: 1527-1535.

Nishiyama Y, Yamamoto H, Allakhverdiev SI, Inaba M, Yokota A, Murata N 2001. Oxidative stress inhibits the repair of photodamage to the photosynthetic machinery. The EMBO journal 20: 5587-5594.
Odum EP 1985. Trends expected in stressed ecosystems. Bioscience 35: 419-422.
OECD. 2008. Test No. 211: Daphnia magna Reproduction Test: OECD Publishing.
OECD. 2006. Test No. 221: Lemna sp. Growth Inhibition Test: OECD Publishing.
Oksanen J, Blanchet F, Friendly M, Kindt R, Legendre P, McGlinn D, Minchin P, O'Hara R, Simpson G, Solymos P. 2016. Vegan: community ecology package. R package version 2.3-5. R Foundation, Vienna, Austria. In.
Parisot F, Bourdineaud J-P, Plaire D, Adam-Guillermin C, Alonzo F 2015. DNA alterations and effects on growth and reproduction in Daphnia magna during chronic exposure to gamma radiation over three successive generations. Aquatic toxicology 163: 27-36.
Pentreath R editor. Protection of the environment from the effects of ionizing radiation. Proceedings of an international conference. 2005.
Pitonzo BJ, Amy PS, Rudin M 1999. Effect of gamma radiation on native endolithic microorganisms from a radioactive waste deposit site. Radiation Research 152: 64-70.
Polikarpov G 1998. Conceptual model of responses of organisms, populations and ecosystems to all possible dose rates of ionising radiation in the environment. Radiation protection dosimetry 75: 181-185.
Preston BL 2002. Indirect effects in aquatic ecotoxicology: implications for ecological risk assessment. Environmental Management 29: 311-323.
Pryakhin E, Mokrov YG, Tryapitsina G, Ivanov I, Osipov D, Atamanyuk N, Deryabina L, Shaposhnikova I, Shishkina E, Obvintseva N 2016. Characterization of biocenoses in the storage reservoirs of liquid radioactive wastes of Mayak PA. Initial descriptive report. Journal of environmental radioactivity 151: 449-460.
Relyea R, Hoverman J 2006. Assessing the ecology in ecotoxicology: a review and synthesis in freshwater systems. Ecology Letters 9: 1157-1171.
Roháček K 2002. Chlorophyll fluorescence parameters: the definitions, photosynthetic meaning, and mutual relationships. Photosynthetica 40: 13-29.
Rohr JR, Kerby JL, Sih A 2006. Community ecology as a framework for predicting contaminant effects. Trends in Ecology & Evolution 21: 606-613.
Rueden CT, Schindelin J, Hiner MC, DeZonia BE, Walter AE, Arena ET, Eliceiri KW 2017. ImageJ2: ImageJ for the next generation of scientific image data. BMC bioinformatics 18: 529.
Shukla A, Parmar P, Saraf M 2017. Radiation, radionuclides and bacteria: An in-perspective review. Journal of environmental radioactivity 180: 27-35.
Strand P, Aono T, Brown J, Garnier-Laplace J, Hosseini A, Sazykina T, Steenhuisen F, Vives i Batlle J 2014. Assessment of Fukushima-derived radiation doses and effects on wildlife in Japan. Environmental Science & Technology Letters 1: 198-203.
Taub F 1989. Standardized aquatic microcosms. Environmental science & technology 23: 1064-1066.
Taub FB 1984. Measurement of pollution in standardized aquatic microcosms. Concepts in Marine Pollution Measurements: 139-158.
Taub FB 1997. Unique information contributed by multispecies systems: examples from the standardized aquatic microcosm. Ecological Applications 7: 1103-1110.
Team RDC. 2017. R Development Core Team: R: a language and environment for statistical computing. Version 3.3.3 Vienna, Austria: R Foundation for Statistical
Computing. In.
Tuovinen TS, Kasurinen A, Häikiö E, Tervahauta A, Makkonen S, Holopainen T, Juutilainen J 2016. Transfer of elements relevant to nuclear fuel cycle from soil to boreal plants and animals in experimental meso-and microcosms. Science of the Total Environment 539: 252-261.
UNSCEAR. 2008. Sources and effects of ionizing radiation In. United Nations Scientific Committee on the Effects of Atomic Radiation
UNSCEAR 2008 Report to the General Assembly, with scientific annexes.
Van Hoeck A, Horemans N, Nauts R, Van Hees M, Vandenhove H, Blust R 2017. Lemna minor plants chronically exposed to ionising radiation: RNA-seq analysis indicates a dose rate dependent shift from acclimation to survival strategies. Plant Science 257: 84-95.

Van Hoeck A, Horemans N, Van Hees M, Nauts R, Knapen D, Vandenhove H, Blust R 2015. Characterizing dose response relationships: chronic gamma radiation in Lemna minor induces oxidative stress and altered polyploidy level. Journal of environmental radioactivity 150: 195-202.

Vandenhove H, Vanhoudt N, Cuypers A, Van Hees M, Wannijn J, Horemans N 2010. Life-cycle chronic gamma exposure of Arabidopsis thaliana induces growth effects but no discernable effects on oxidative stress pathways. Plant Physiology and Biochemistry 48: 778-786.

Vermaat J 2005. Periphyton dynamics and influencing factors. Periphyton ecology, exploitation and management. Cambridge: CABI Publishing: 35-49.

Wullschleger EB, Jokela J 2002. Morphological plasticity and divergence in life-history traits between two closely related freshwater snails, Lymnaea ovata and Lymnaea peregra. Journal of Molluscan Studies 68: 1-5.

Yousef Y, Padden T, Gloyna E 1975. Diurnal changes in radionuclides uptake by phytoplankton in small scale ecosystems. Water Research 9: 181-187.

Zuur AF, Ieno EN, Walker NJ, Saveliev AA, Smith GM. 2009. GLM and GAM for count data. In. Mixed effects models and extensions in ecology with R: Springer. p. 209-243.

Supplementary Information

Table S1: Species list of the phytoplankton community

Class	Species
Eustigmatophyceae	*Eustigmatos* magnus
Chlorophyceae	*Raphidocelis subcapitata* *Langerheimia* sp
Bacillariophyceae	*Cyclotella* sp *Navicula* sp
Ciliophora	*Euplotes* sp *Rimostrombidium* sp
Euglenozoa	*Peranema* sp

Table S2. Abiotic parameters (mean ± st.dev). based on measurements taken with a WTW Multimeter 350

Average dose rate	n	t0			t10			t21			All time points		
Conductivity (µS/cm)													
0.004 mGy/h	5	150.72	±	22.26	163.06	±	18.10	191.94	±	15.93	168.57	±	21.16
0.72 mGy/h	6	170.73	±	31.96	179.82	±	25.38	208.63	±	23.71	186.39	±	19.79
1.78 mGy/h	4	129.88	±	22.07	149.83	±	18.03	184.40	±	14.12	154.70	±	27.59
7.85 mGy/h	2	170.55	±	33.30	181.75	±	27.22	211.15	±	23.83	187.82	±	20.97
18.5 mGy/h	2	143.65	±	44.05	157.80	±	35.36	189.20	±	32.24	163.55	±	23.31
all dose rates	19	153.99	±	30.21	166.98	±	23.98	197.36	±	21.25			
Temperature (°C)													
0.004 mGy/h	5	19.14	±	0.13	18.30	±	0.10	18.76	±	0.11	18.7	±	0.42
0.72 mGy/h	6	19.18	±	0.04	18.22	±	0.04	18.52	±	0.10	18.64	±	0.49
1.78 mGy/h	4	19.18	±	0.05	18.00	±	0.08	18.53	±	0.10	18.57	±	0.59
7.85 mGy/h	2	19.25	±	0.07	18.15	±	0.07	18.70	±	0.00	18.70	±	0.55
18.5 mGy/h	2	19.25	±	0.07	18.20	±	0.14	18.75	±	0.07	18.73	±	0.53
all dose rates	19	19.18	±	0.08	18.18	±	0.13	18.63	±	0.14			
pH													
0.004 mGy/h	5	7.00	±	0.09	7.20	±	0.16	7.32	±	0.21	7.18	±	0.16
0.72 mGy/h	6	7.03	±	0.06	7.21	±	0.07	7.24	±	0.09	7.16	±	0.12
1.78 mGy/h	4	6.98	±	0.07	7.17	±	0.08	7.21	±	0.13	7.12	±	0.12
7.85 mGy/h	2	7.05	±	0.02	7.16	±	0.09	7.22	±	0.07	7.14	±	0.09
18.5 mGy/h	2	7.04	±	0.11	7.21	±	0.01	7.25	±	0.01	7.16	±	0.11
all dose rates	19	7.01	±	0.07	7.19	±	0.10	7.26	±	0.13			
Light (lux)													
0.004 mGy/h	5	1144	±	150									
0.72 mGy/h	6	1204	±	118									
1.78 mGy/h	4	1229	±	124									
7.85 mGy/h	2	1184	±	46									
18.5 mGy/h	2	1216	±	168									
all dose rates	19	1192	±	119									

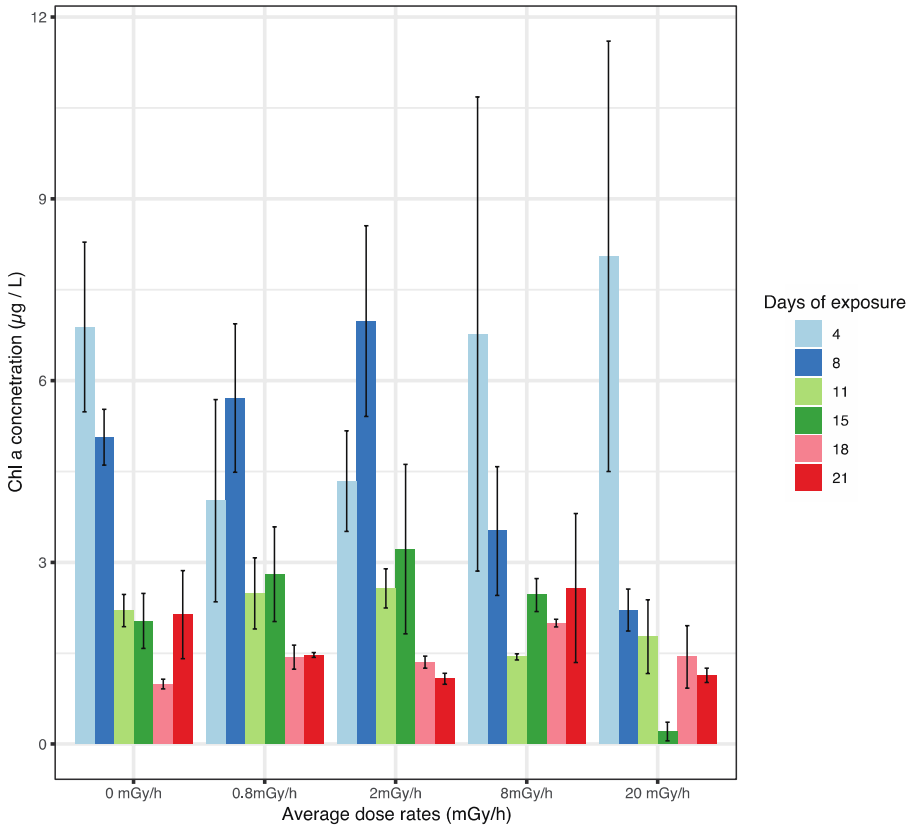

Figure S1: Average chlorophyll a concentrations per dose rate per sampling day throughout the 21 day exposure.